TMF: fatica termo-meccanica

Lecture 15

Meccanismo

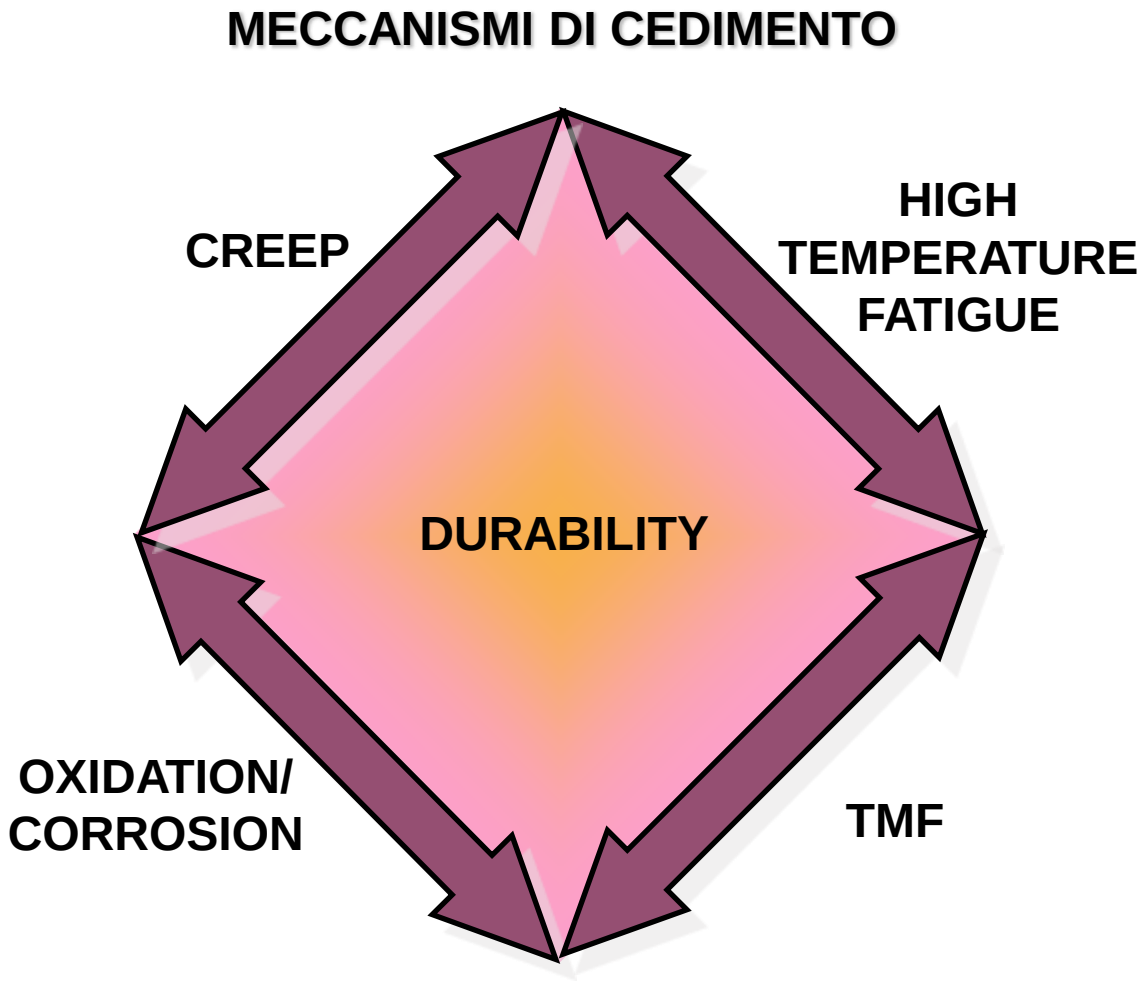
MECCANISMI DI CEDIMENTO
CREEP
HIGH TEMPERATURE FATIGUE
DURABILITY
OXIDATION/ CORROSION
TMF

Meccanismo

TMF

gradienti termici + sollecitazioni meccaniche cicliche

CICLO ISOTERMO (HTLCF)

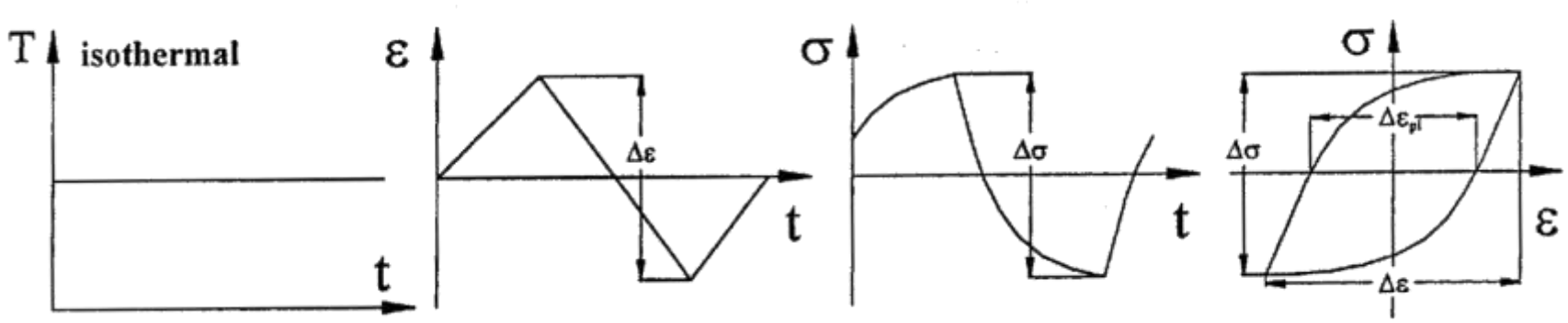

- Ciclo simmetrico in deformazione e sforzo

Meccanismo

TMF

gradienti termici + sollecitazioni meccaniche cicliche

CICLO IP

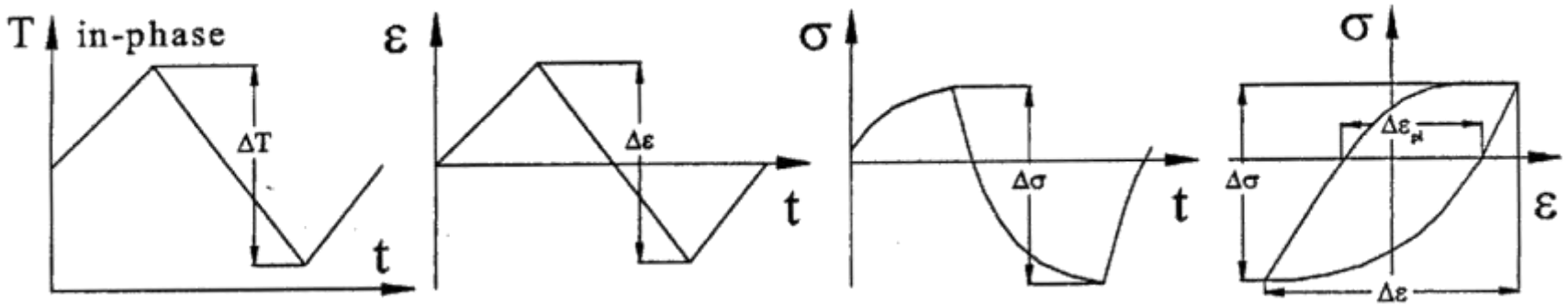

- Tensione media di compressione

La trazione massima si raggiunge a temperature più alte a cui il materiale esibisce una minore resistenza. Conseguenza l'area del ciclo a trazione è minore di quella a compressione

Meccanismo

TMF

gradienti termici + sollecitazioni meccaniche cicliche

CICLO OP

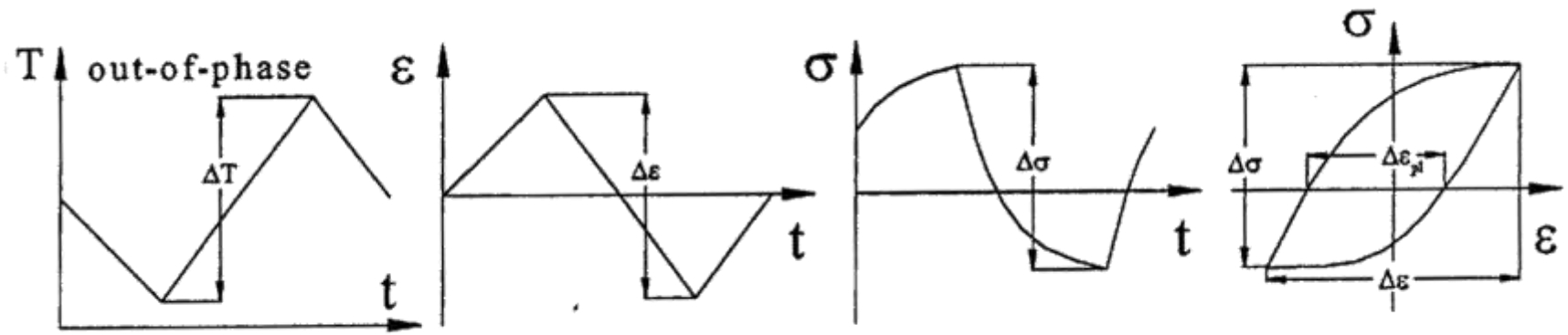

- Presenza di una tensione media di trazione anche per R_ε=-1

L'ampiezza della tensione media dipende dal materiale, angolo di fase, intensità del ciclo termico

Meccanismo

CICLO A DIAMANTE LINEARIZZATO

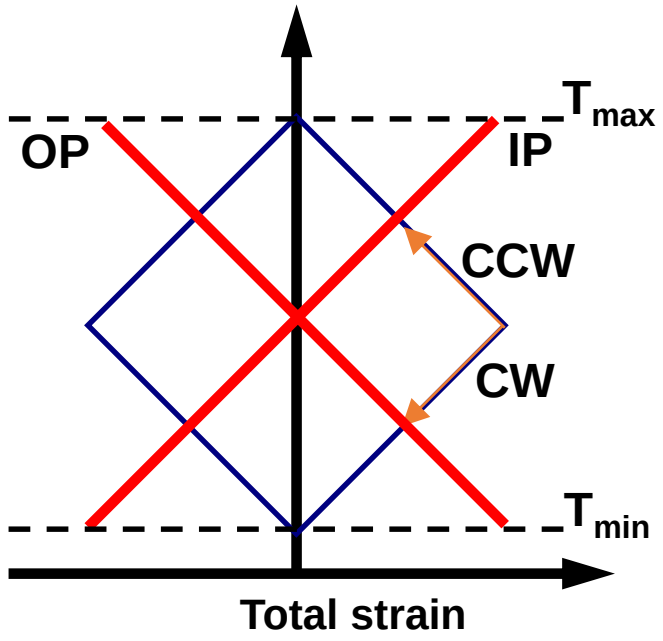

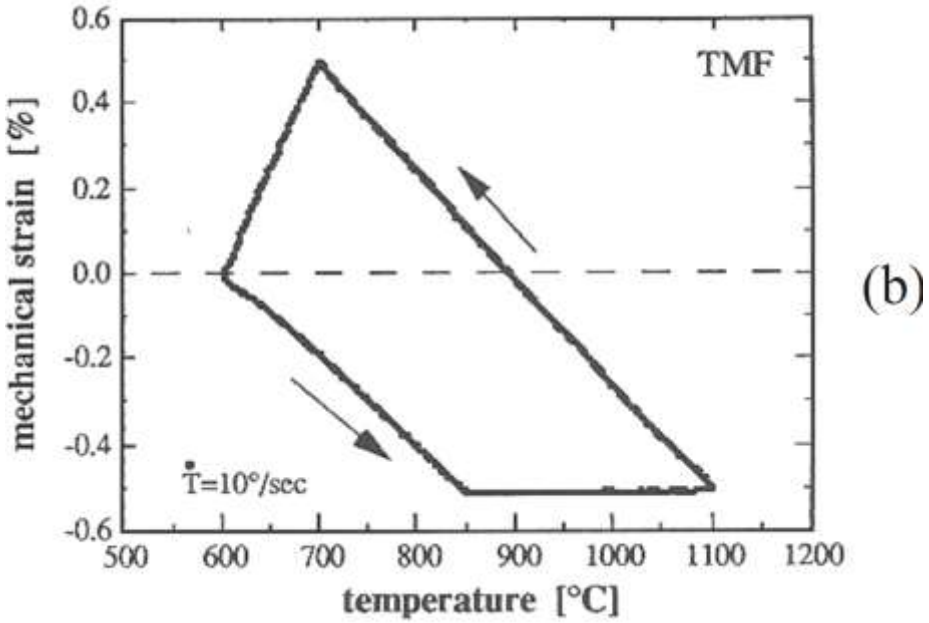

(b)

Meccanismo

Assenza di isteresi nel ciclo stabilizzato
Effetto “tensione media”
La sensibilizzazione sembra essere il parametro di controllo per la durata

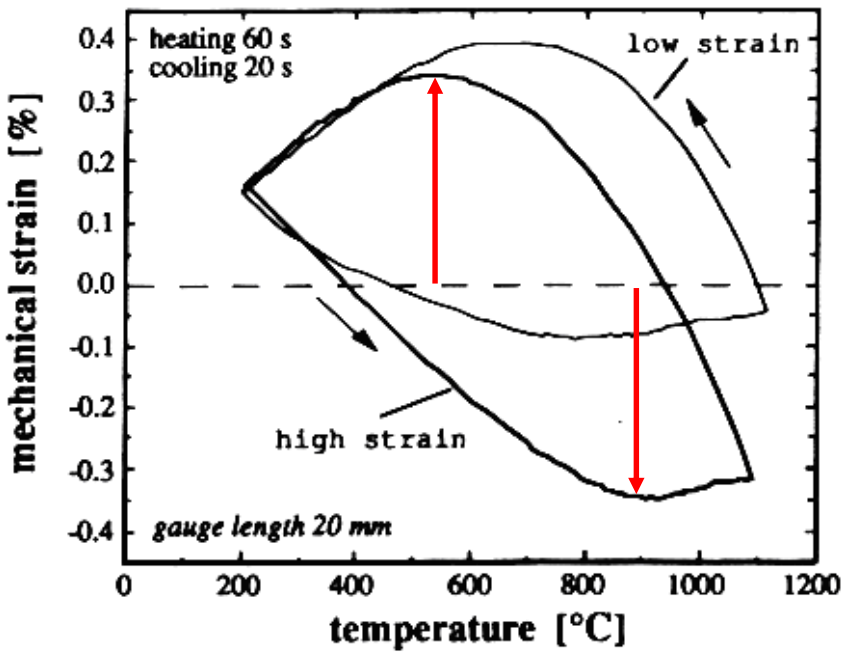

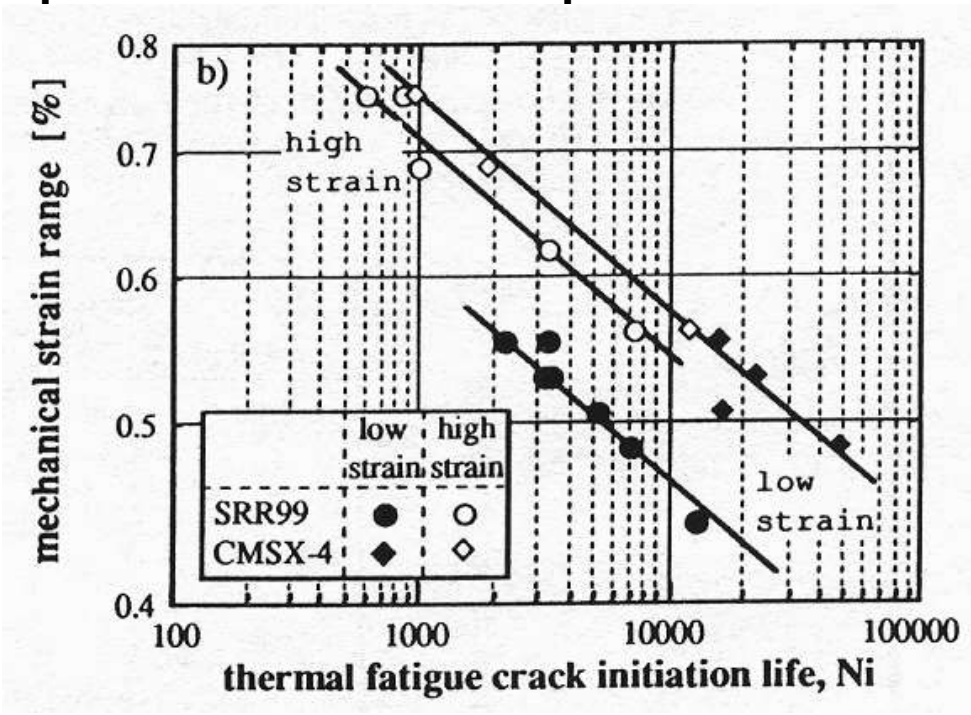

Meccanismo

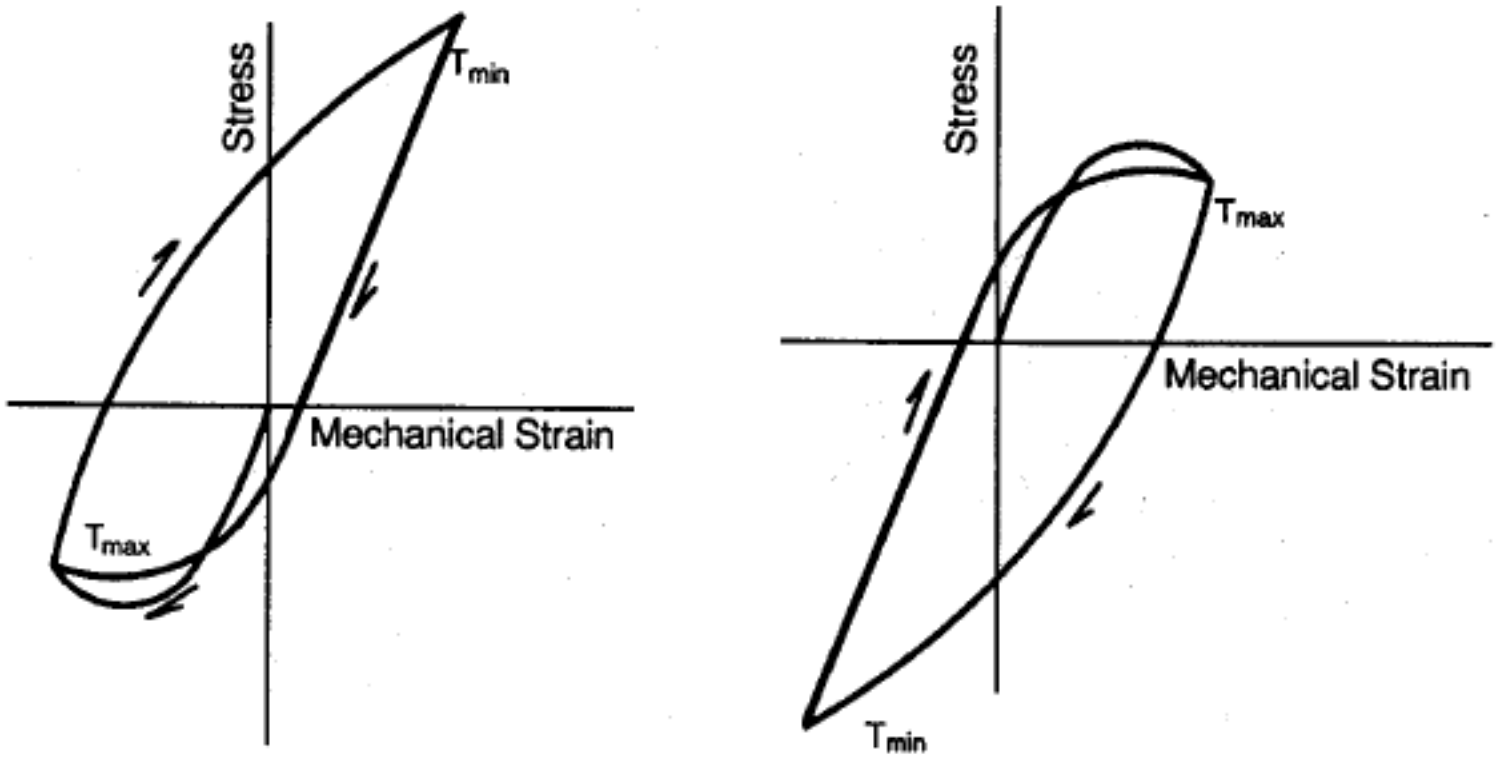

Out-of-Phase In-Phase

Figure 1 Load and Temperature Phasing

Modellazione

$$\frac{1}{N_f} = \frac{1}{N_f^{fatigue}} + \frac{1}{N_f^{oxidation}} + \frac{1}{N_f^{creep}}$$

Meccanismi

High temperature fatigue mechanisms
Fatigue damage in the life regime of interest in TMF is in the form of nucleation and growth of microcracks.

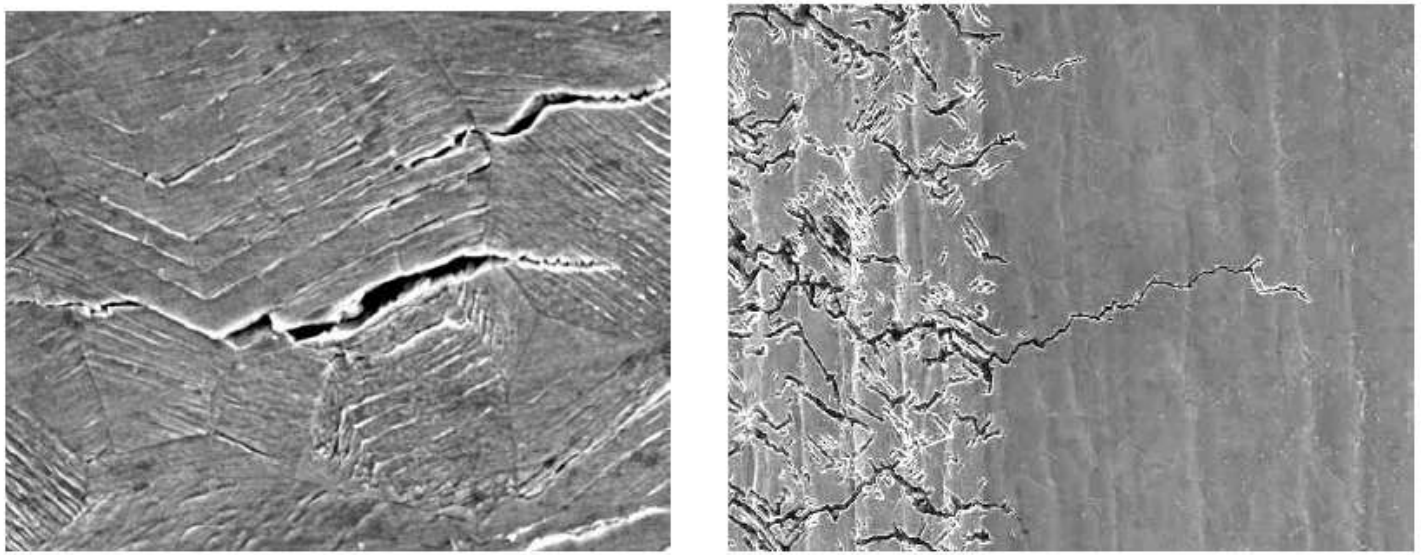

surface view cross section view

FIGURE 3 Formation of Surface Cracks in 20-25 Austenitic Steel [3]

Meccanismi

High temperature fatigue mechanisms

Microcrack density will decrease at lower strain levels.

Many microcracks nucleate on the surface and a few of them are able to penetrate into the bulk of the material.

The process is driven by cyclic plastic strains where oxidation and creep effects are negligible.

Fatigue damage will dominate at high strain ranges, strain rates and low temperatures.

Meccanismi

Oxidation mechanisms

Oxidation damage can occur in the form of an oxide intrusion

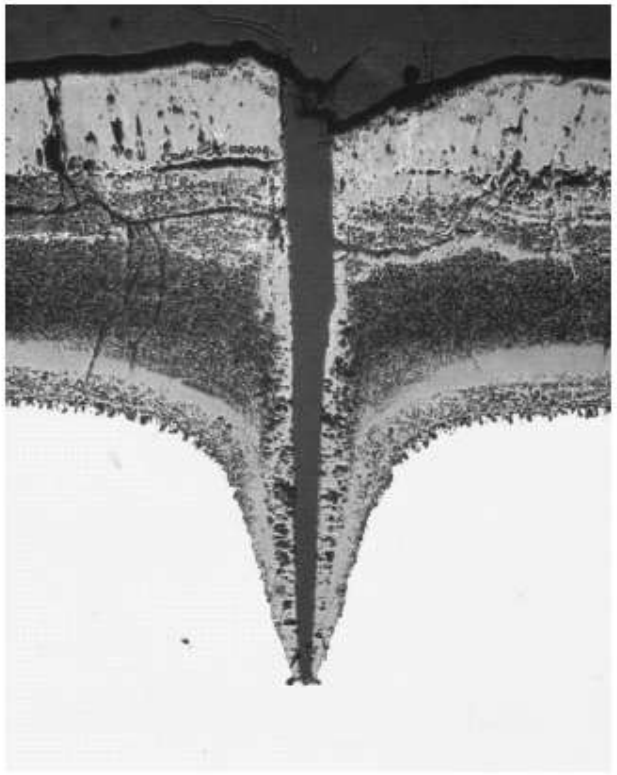

Figure 4 Oxidation Damage in Steel [4]

Meccanismi

Oxidation mechanisms

In OP loading, an oxide layer can form on the surface when the material is hot and in compression.

At the lower temperature the oxide layer becomes brittle. During mechanical straining it then cracks to expose new clean metal surfaces.

This clean metal will rapidly oxidize and the process repeats during the next mechanical strain cycle.

Oxide cracks can also form during IP loading. In this case, the oxide forms during the hot portion of the loading cycle while the material is in tension. Then upon cooling the oxide film undergoes a buckling delamination.
Oxide formation and rupture during isothermal loading is not the dominant failure mechanism and is not reflected in isothermal test or materials data.

Oxide formation will occur easier and faster at higher temperatures.

Meccanismi

Creep mechanisms

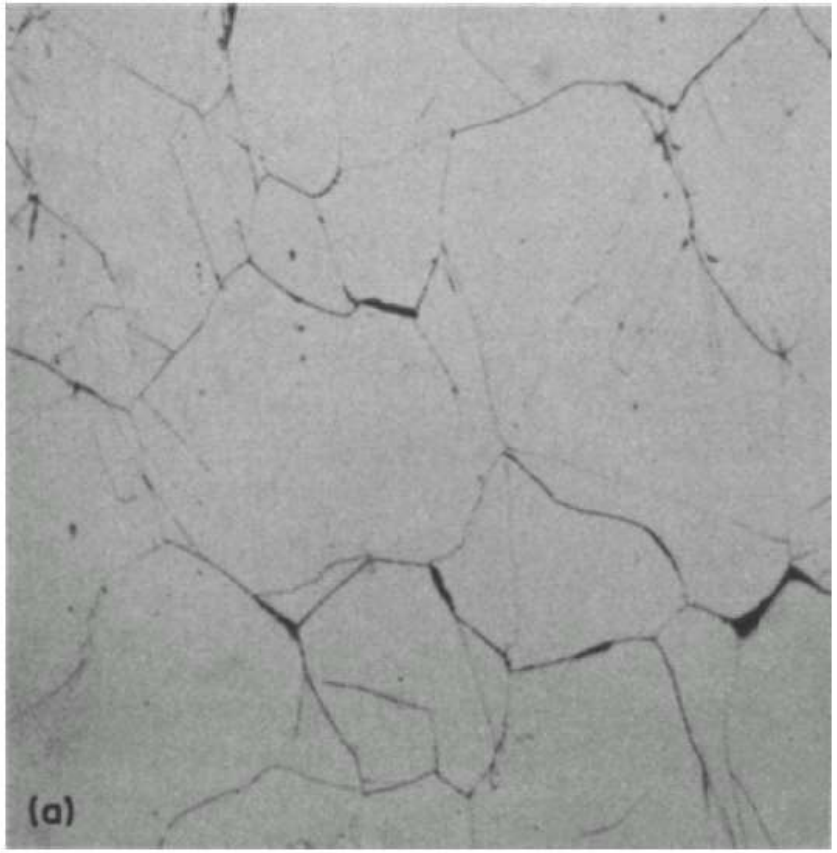

Figure 5 Wedge crack nucleation in Type 316 stainless steel [5]

Meccanismi

Creep mechanisms

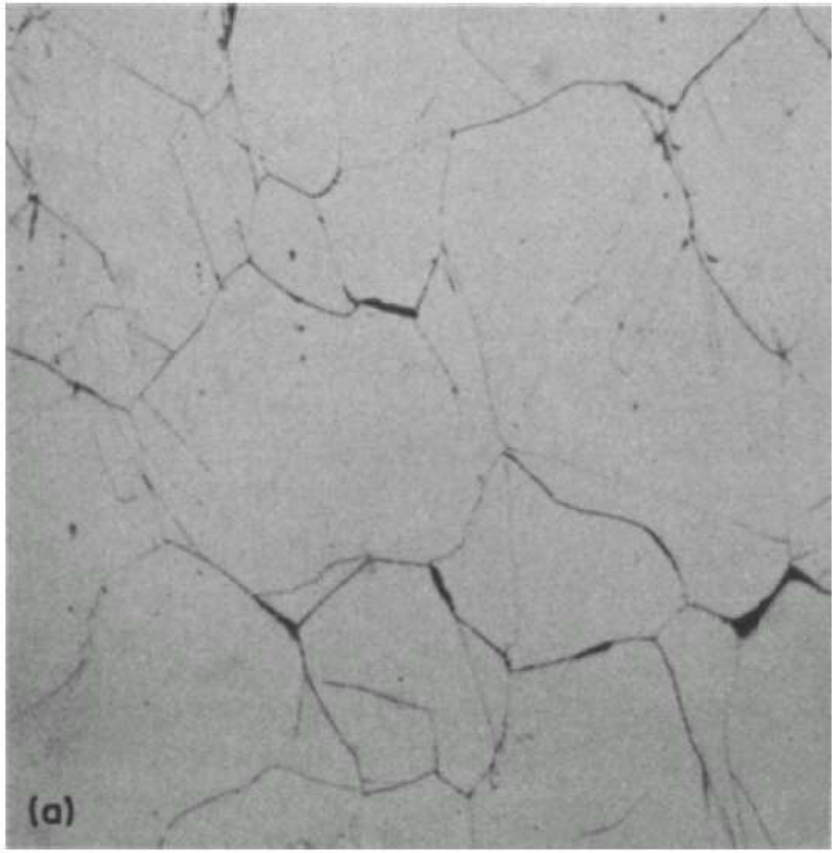

Figure 5 Wedge crack nucleation in Type 316 stainless steel [5]

Modellazione

Fatigue mechanisms

$$\frac{\Delta\varepsilon}{2} = \frac{\sigma_f'}{E}\left(2N_f^{\text{fatigue}}\right)^b + \varepsilon_f'\left(2N_f^{\text{fatigue}}\right)^c$$

σ_f'	fatigue strength coefficient
b	fatigue strength exponent
ε_f'	fatigue ductility coefficient
c	fatigue ductility exponent
E	elastic modulus

Modellazione

Oxidation mechanisms

Oxidation damage is a function of the strain range, strain rate, and temperature.

A phasing factor is introduced to account for the type of oxide cracking that occurs in either IP or OP loading.

Phasing is represented by the ratio of thermal and mechanical strain rates.

Oxidation rate is determined by the effective parabolic oxidation constant

$$\text{if } \Delta\varepsilon_{mech} > \varepsilon_0 \qquad \frac{1}{N_f^{oxidation}} = \left[\frac{H_{cr}}{\Phi^{ox} K_{peff}}\right]^{\frac{1}{\beta}} \frac{2\left(\Delta\varepsilon_{mech}\right)^{\frac{2}{\beta}+1}}{\dot{\varepsilon}^{1-\frac{b}{\beta}}}$$

Modellazione

Oxidation mechanisms

$$\Phi_{ox} = \frac{1}{t_c}\int_0^{t_c} \phi_{ox}\, dt$$

$$\phi_{ox} = \exp\left[-\frac{1}{2}\left(\frac{\dot{\varepsilon}_{th}/\dot{\varepsilon}_{mech}+1}{\xi^{ox}}\right)^2\right]$$

ε_o threshold strain for oxide cracking
H_{cr} constant related to critical oxide thickness
β mechanical strain range exponent
b thermal strain rate sensitivity exponent

ξ^{ox} oxidation phasing constant for thermal and mechanical strains

$$K_{peff} = \int_0^{t_c} D_0 \exp\left(\frac{-\Delta H^{ox}}{RT}\right) dt$$

ΔH^{ox} activation energy for oxidation
D_o scaling constant for oxidation

Modellazione

Creep mechanisms

Creep damage is a function of the stresses, time and temperature.

Microstructural creep damage differs in tension and compression.

It is commonly assumed that microcracks do not form and grow in compression.

$$\frac{1}{N_f^{creep}} = \int_0^{t_c} A_{cr} \Phi^{cr} \exp\left(\frac{-\Delta H^{cr}}{RT}\right)\left(\frac{\alpha_1 \bar{\sigma} + \alpha_2 \sigma_h}{K}\right)^m$$

ΔH^{cr}	activation energy for creep
A_{cr}	scaling constant for creep
m	creep stress exponent
α_1	stress state constant
α_2	hydrostatic stress sensitivity constant

Modellazione

Creep mechanisms

If no creep damage occurs in compression α1 = 1/3 and α2 = 1. Here, K is the drag
stress which will be defined in the next section. A phasing factor φcr is also introduced to account for different creep damage mechanisms such as intergranular or transgranular cracking

$$\Phi_{cr} = \frac{1}{t_c}\int_0^{t_c} \phi^{cr} dt$$

$$\phi_{cr} = \exp\left[-\frac{1}{2}\left(\frac{\dot{\varepsilon}_{th}/\dot{\varepsilon}_{mech} - 1}{\xi^{cr}}\right)^2\right]$$

Modellazione

Strain range partitioning. SRP

The SRP life prediction model partitions the inelastic strain-range into time-independent plasticity and time-dependent creep, rather than working with the total inelastic strain-range alone.

Each component contributes a certain fraction to the total damage.

Under cyclic reversed loading, there are four possible combination cycles of inelastic strain, which the SRP model needs to consider.

Modellazione

Strain range partitioning. SRP

PP – plasticità in tensione e compressione

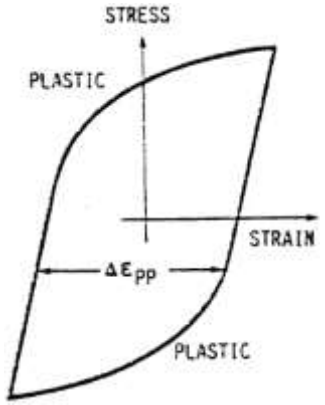

CP – creep in tensione e plasticità in compressione

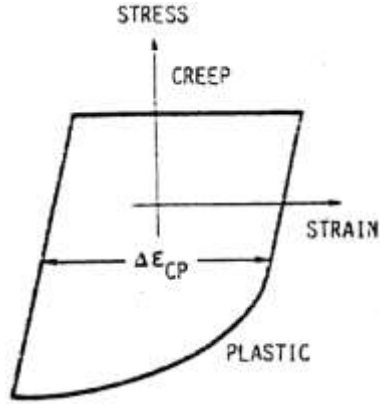

PC – creep in tensione e compressione

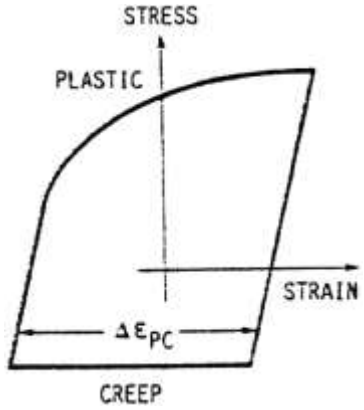

CC – creep in tensione e compressione

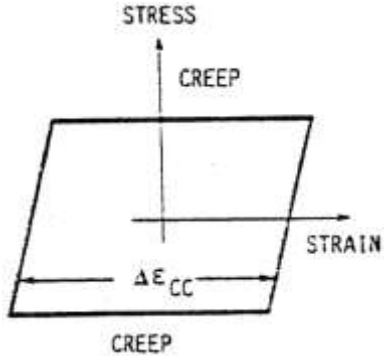

Modellazione

Strain range partitioning. SRP

$$\frac{1}{N_f} = \frac{1}{N_{pp}} + \frac{1}{N_{cc}} + \frac{1}{N_{pc}} + \frac{1}{N_{cp}}$$

Manson, Halford and Hirschberg 1971.

$$\frac{1}{N_f} = \frac{F_{pp}}{N'_{pp}} + \frac{F_{cc}}{N'_{cc}} + \frac{F_{pc}}{N'_{pc}} + \frac{F_{cp}}{N'_{cp}}$$

Manson and Halford

F_{pp}, F_{cc}, F_{pc}, and F_{cp} are PP, CC, PC and CP strain-range fractions, for example, $F_{pp} = \Delta\varepsilon_{pp}/\Delta\varepsilon_{in}$. N'_{pp}, N'_{cc}, N'_{pc} and N'_{cp} are the fatigue lives produced by PP, CC, PC and CP inelastic strain cycles respectively, but they are calculated according to equations (13)-(16) using total inelastic strain range, $\Delta\varepsilon_{in}$ rather than the partitioned inelastic strain-range components ($\Delta\varepsilon_{pp}$, $\Delta\varepsilon_{cc}$, $\Delta\varepsilon_{pc}$ and $\Delta\varepsilon_{cp}$).

Modellazione

Strain range partitioning. SRP

One of the advantages of the SRP rule is that it is relatively temperature independent (Halford, Hirschberg and Manson, 1973).

The life relationships are governed by the four inelastic strain-ranges and not greatly affected by the temperature at which the strains are imposed.

If particular strain-ranges are imposed at one temperature, the life will be similar to that when the same strain-ranges of the same type are applied at another temperature.

Modellazione

Strain range partitioning. SRP

To obtain the four unique partitioned strain-range vs. cyclic life relationships, four separate PP, PC, CC and CP creep-fatigue tests have to be done (refer to Figs 2 and 3 of Halford, Hirschberg and Manson, 1973). Results of these tests are fitted to the Coffin-Manson Equation (6), and can expressed as:

$$\Delta\varepsilon_{pp} = A_{pp}\,(N_{pp})^{C_{pp}} \tag{13}$$

$$\Delta\varepsilon_{pc} = A_{pc}\,(N_{pc})^{C_{pc}} \tag{14}$$

$$\Delta\varepsilon_{cp} = A_{cp}\,(N_{cp})^{C_{cp}} \tag{15}$$

$$\Delta\varepsilon_{cc} = A_{cc}\,(N_{cc})^{C_{cc}} \tag{16}$$

The coefficients A and exponents C are experimentally determined material constants.